The *MicroRNA397b-LACCASE2* Module Regulates Root Lignification under Water and Phosphate Deficiency[1]

Hitaishi Khandal, Amar Pal Singh, and Debasis Chattopadhyay[2,3]

National Institute of Plant Genome Research, Aruna Asaf Ali Marg, New Delhi 110067, India

ORCID IDs: 0000-0002-3899-4325 (H.K.); 0000-0002-5754-4987 (D.C.).

Deficiency of water and phosphate induce lignin deposition in roots. LACCASEs, a family of cell wall-localized multicopper oxidases, are involved in lignin biosynthesis. We demonstrate here that LACCASE2 (LAC2) acts as a negative regulator of lignin deposition in root vascular tissues during water deficit. An Arabidopsis (*Arabidopsis thaliana*) transfer DNA insertion mutant of *LAC2* displayed a short primary root and high lignin deposition in root vascular tissues. However, restoration of *LAC2* expression rescued these phenotypes. *LAC2* expression was significantly down-regulated under water deficit and posttranscriptionally regulated by microRNA397b (miR397b) in roots under normal and water-deficit conditions. Down-regulation of miR397b activity increased *LAC2* expression and root length, and decreased lignin content in root vasculature. Similarly, phosphate (Pi) deficiency inversely affected *miR397b* and *LAC2* expression. Lignin deposition in the root elongation zone under Pi-limited conditions was dependent on *LAC2* expression. Localized iron accumulation and callose deposition in the root elongation zone under Pi deficiency increased with LAC2-dependent lignification, suggesting a direct relationship between these processes. Our study reveals a regulatory role for the *miR397b-LAC2* module in root lignification during water and phosphate deficiency.

Environmental conditions such as water and nutrient availability are the major limiting cues for plant growth and productivity (Boyer, 1982; Bohnert et al., 1995). Differential availability of natural resources elicits developmental plasticity of plant roots to facilitate acquisition of nutrients and water from the soil for sustenance of the plant (van Kleunen and Fischer, 2005; Valladares et al., 2007). Water uptake through the roots during water deficiency is insufficient to maintain physiological and biochemical processes to support growth and development of the plant. Therefore, how root development is regulated under water and nutrient deficit is a subject of considerable interest in agriculture (Sharp et al., 1988; Sinclair and Muchow, 2001). Water deficit inhibits primary root growth particularly at the elongation zone (EZ; Sharp et al., 1988; Fraser et al., 1990; Pritchard, 1994; Bao et al., 2014), and this is one of the important factors that determine the overall root growth in plants during water deficiency. Inhibition of cell elongation in the root EZ in some plants has been shown to accompany chemical modification of the cell wall and stellar accumulation of cell wall phenolics, particularly lignin (Fan et al., 2006). Increased expression of lignin biosynthetic genes in rice (*Oryza sativa*) roots under water deficit has been reported (Yang et al., 2006). A relatively salt-tolerant wheat variety (*Triticum aestivum*) exhibited more lignification in root cells compared to the salt-sensitive variety, while exposure to salinity also intensified lignin deposition in the cowpea (*Vigna unguiculata*) root cell wall (Jbir et al., 2001; Maia et al., 2013).

Lignins are deposited in various tissues and cells, predominantly in secondary cell walls of fiber, ray parenchyma, vessels, and the vascular bundle sheath (Zhou et al., 2011; Yamamura et al., 2013). The main function of cell wall lignification is to strengthen the plant vascular body, and it involves deposition of phenolic polymers on extracellular polysaccharide matrix (Ros Barceló, 1997). Lignins are hydrophobic, and therefore, lignified xylem cell walls are thought to be less permeable to water, thus preventing water leakage and helping transport water and nutrients (Hatfield and Vermerris, 2001; Reina et al., 2001; Kitin et al., 2010).

Inorganic phosphate (Pi) is one of the major limiting nutrients in the natural soil. Low Pi inhibits primary root elongation and increases lateral root density to enhance root-to-soil surface contact for Pi acquisition (Raghothama, 1999). To cope with suboptimal Pi conditions, plants adopt two major strategies, the systemic response and the local response. The systemic response

[1]This work was supported by grants from the Department of Biotechnology (DBT), Ministry of Science and Technology, Government of India (BT/PR3304/AGR/2/815/2011 and BT/HRD/35/01/03/2014) and the National Institute of Plant Genome Research (NIPGR), New Delhi, India.

[2]Author for contact: debasis@nipgr.ac.in.

[3]Senior author.

The author responsible for distribution of materials integral to the findings presented in this article in accordance with the policy described in the Instructions for Authors (www.plantphysiol.org) is: Debasis Chattopadhyay (debasis@nipgr.ac.in).

D.C. and A.P.S. conceived the research plans, supervised the experiments, and interpreted the results; D.C. conceived the project and wrote the article with contributions from all the authors; and H.K. performed all the experiments. All authors read, corrected, and approved the manuscript.

www.plantphysiol.org/cgi/doi/10.1104/pp.19.00921

involves increased Pi uptake and metabolic adjustment to optimize Pi utilization. In the case of local response, roots undergo striking morphological and developmental changes, such as primary root growth arrest, development of lateral roots, and root hairs (López-Bucio et al., 2002; Abel S, 2011; Péret et al., 2011; Singh et al., 2014). Response to Pi starvation in Arabidopsis (*Arabidopsis thaliana*) is accompanied by induced lignification in the primary root EZ (Ziegler et al., 2016), indicating a relationship between Pi limitation, root lignifications, and primary root growth arrest.

Lignins, the second most abundant biopolymers in nature, are complex three-dimensional heterogeneous molecules composed of a network of phenylpropanoid units (Higuchi, 1985). The phenolic units are biosynthesized from Phe that undergoes a series of chemical modifications within the cytosol using various enzymes to produce *p*-coumaryl alcohol, coniferyl alcohol, and sinapyl alcohol (Vanholme et al., 2010). These monomeric precursors of lignins (monolignols) are transported to the cell wall, where they are polymerized and amalgamated in the cell wall (Nilsson et al., 2010; Liu et al., 2011). Cell wall-localized PEROXIDASEs and LACCASEs (*p*-diphenol:oxygen oxidoreductase, EC1.10.3.2) catalyze the formation of monolignol radicals by oxidation and facilitate polymerization of monolignols to complex lignins (Sarkanen, 1971; Vanholme et al., 2010).

Extracellular glycoprotein LACCASEs are multicopper oxidases and use oxygen as a substrate to reversibly catalyze formation or degradation of various phenolic, inorganic, and aromatic amine polymers (Reinhammar and Malmstroem, 1981). Degradation of lignin by fungal and bacterial LACCASEs has been demonstrated (Youn et al., 1995; de Gonzalo et al., 2016). Involvement of plant LACCASEs in lignification was proposed due to their ability to oxidize monolignol in vitro (Higuchi and Ito, 1958; Freudenberg, 1959; Takahama, 1995) and to detection of LACCASE-like activity in lignifying cell walls of differentiating xylems (Driouich et al., 1992; McDougall, 2000; Richardson et al., 2000). Subsequently, complementary DNAs (cDNAs) of some *LACCASE*s were cloned from a differentiating xylem cDNA library (Ranocha et al., 1999). Antisense suppression of *LAC3*, *LAC90*, or *LAC110* expression resulted in altered lignin content in the xylem fiber cell wall of Poplar (*Populus trichocarpa*; Ranocha et al., 2002). Simultaneous disruption of *LAC4* and *LAC17* in Arabidopsis resulted in reduced stem lignin content, and the *lac4lac17lac11* triple mutant showed severe arrest in plant growth and vascular development, with an apparent lack of lignification in root vascular tissue (Berthet et al., 2011; Zhao et al., 2013). LACCASE4 and LACCASE17 were shown to localize at the secondary cell walls throughout the protoxylem tracheary element and were able to catalyze lignin polymerization using exogenously supplied monolignols (Schuetz et al., 2014). However, our knowledge about how lignification is regulated in the primary root elongation-differentiation zone during abiotic stresses and how it contributes to root developmental plasticity is still scant. In this report, we have investigated the posttranscriptional regulation of *LACCASE2* gene expression by *microRNA397b* (*miR397b*) and its implication in lignification in root vascular tissue in response to water and phosphate limitation.

RESULTS

LAC2 Negatively Regulates Root Lignification during Water Deficit

To investigate the effect of water deficit on primary root length, Arabidopsis ecotype Columbia (Col-0) plants at 4 d post germination (dpg) were treated with 0.4 M mannitol. Primary root growth was inhibited in mannitol-treated plants compared to untreated plants, and the inhibition was significant within 48 h (Fig. 1A). To investigate lignin deposition after 48 h of mannitol treatment, treated and untreated roots were stained with basic fuchsin. Early cell differentiation and intense lignification in protoxylems and metaxylem poles, which are indicators of secondary cell wall formation, were observed within 4–5 cells and 6–7 cells above the EZ boundary in the mannitol-treated samples (Fig. 1B). Similar alteration in root xylem patterning following abscisic acid (ABA) treatment was reported before (Ramachandran et al., 2018; Bloch et al., 2019). A low level of lignin deposition in the endodermis was also visible. Quantitative analysis of the total lignin content showed that it was >4-fold higher in mannitol-treated roots compared to untreated roots (Fig. 1C). Relative fold expression of all the seventeen *LACCASE* genes in Col-0 roots upon mannitol treatment at different time points up to 48 h showed a consistent decrease in expression of two *LACCASEs*, *LAC2* and *LAC4* (Fig. 1D; Supplemental Fig. S1). Of these, *LAC2* showed the greatest decline, 12-fold after 12 h and >4-fold at the end of this treatment. Earlier, a microarray-based expression analysis of *Arabidopsis LACCASE* genes under various abiotic stresses reported a >4-fold decrease in expression of *LAC2* under osmotic, dehydration, and heat treatments (Toufighi et al., 2005).

To investigate the role of *LAC2* in root lignin deposition, primary root length of 14-dpg seedlings of two *LAC2* transfer DNA (T-DNA) insertion lines (SALK_025690C and SAIL_292_B04) were measured. Both the mutants displayed ~1.4- to 1.5-fold shorter root length compared to the Col-0 plants under normal growth conditions (Fig. 2, A and B). To explore the extent of lignin deposition in the mutant roots, 14-dpg mutant seedlings were stained with basic fuchsin. An intensified lignification was observed mostly in the metaxylem poles of the roots of mutant seedlings, suggesting escalated metaxylem differentiation (Fig. 2, C and D). Comparison of the accumulation of cell wall-associated phenolics by UV-induced autofluorescence showed an intense autofluorescence, indicating highly

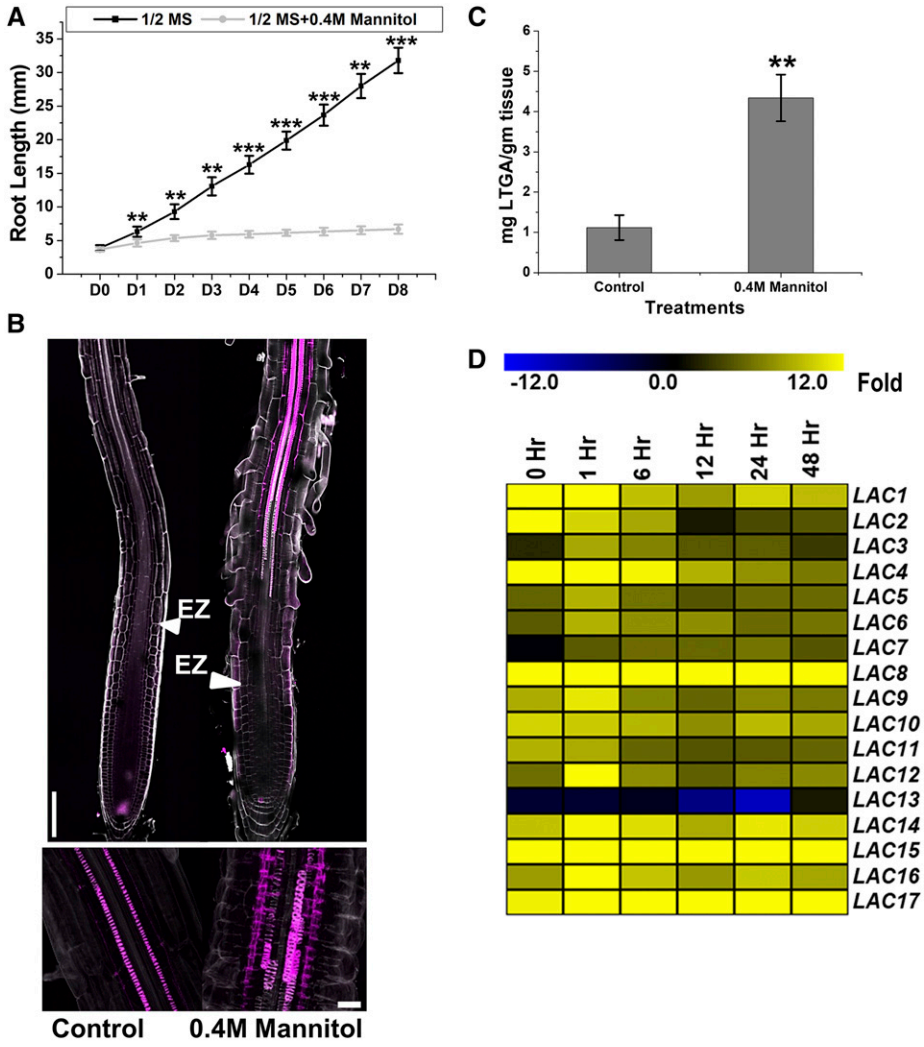

Figure 1. Root growth arrest, lignin deposition, and *LACCASE* expression in Arabidopsis roots during water deficit. A, Primary root length of Col-0 seedlings upon transfer of 4 dpg seedlings (D0) to medium without and with 0.4 M mannitol for 8 d (D0–D8). Root lengths were measured using ImageJ tool and represent data from triplicate experiments ($n = 15$ per replicate). Error bars represent the mean ± SE. Asterisks indicate values that are significantly different from their equivalent control as determined by Student's *t* test (*$P < 0.05$; **$P < 0.01$; ***$P < 0.001$). 1/2 MS, One-half strength MS medium. B, Roots of 4-dpg Col-0 seedlings were treated without (Control) and with 0.4 M mannitol for 48 h and were stained with basic fuchsin and calcofluor white after the treatment for visualization of lignin at 20× magnification (scale bar = 50 μm). The lower images are 63× magnifications of root vascular tissue at 8–10 cells above the initiation of the EZ. Scale bar = 10 μm. C, Estimation of total root lignin content of Col-0 seedlings treated as above, without (Control) and with 0.4 M mannitol for 48 h, using the thioglycolic acid method. Lignin estimation was done in three biological replicates ($n = 15$ per replicate). D, At 4 dpg Col-0 seedlings were treated with 0.4 M mannitol for different time periods up to 48 h, and expression of *LACCASE* genes in roots was analyzed. Transcript abundance of each *LACCASE* gene is presented as a value (Fold) normalized with that of *AtACTIN2* (At3g18780) at that time point of treatment and presented as heat maps using TIGR Multi Experiment Viewer (version 4.9). Values in the heat map represent mean values of three biological replicates. A bar diagram of relative fold expression values is presented in Supplemental Figure S1.

lignified protoxylem and metaxylem poles in the roots of the SALK mutant line (Fig. 2, E and F). In agreement with the fuchsin staining and autofluorescence, total root lignin content in the mutant seedlings was ~1.7- to 1.8-fold higher than in the Col-0 seedlings (Fig. 2G). All these observations suggested that LAC2-associated root xylem differentiation and lignification could be an important factor behind the shorter roots in these mutants, although the possibility that increase in lignin deposition and decrease in root growth are two independent processes cannot be ruled out. As the SALK_025690C showed higher root lignin content, this mutant was used for further experiments and was referred to as *lac2*. Interestingly, the root lengths of Col-0 and the *lac2* mutant are similar up to 6 dpg (Supplemental Fig. S2A); the difference in root growth appeared thereafter. To examine the possible involvement of other LACCASEs in lignification in the *lac2*

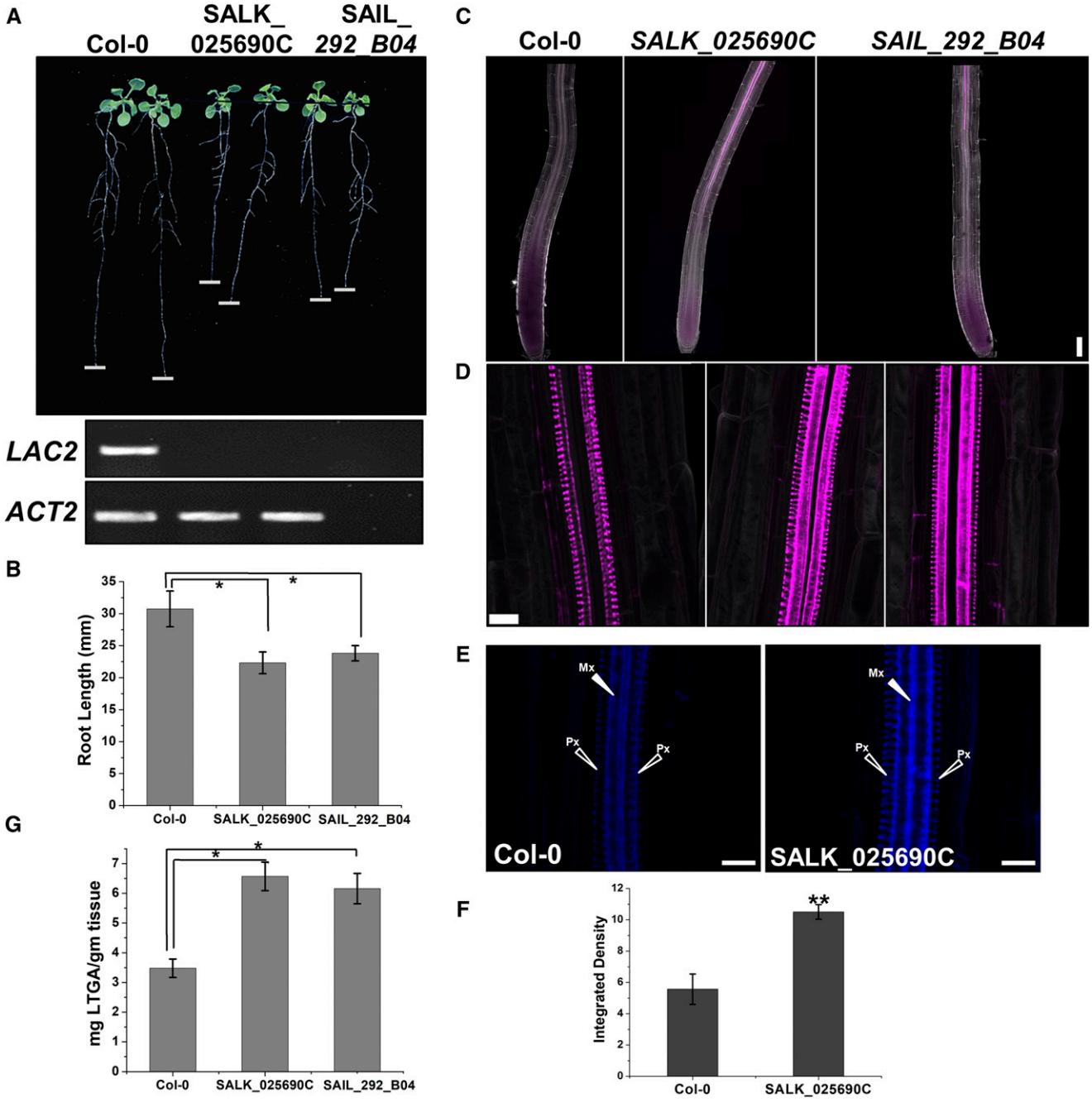

Figure 2. The short root phenotype of *lac2* mutants is accompanied by enhanced lignin deposition in root vasculature. A, Comparison of the primary root phenotypes in 14-dpg Col-0 and *lac2* mutants SALK_025690C and SAIL_292_B04 under normal growth conditions. Lower images show *LACCASE2* and *ACT2* gene expressions in the above lines as determined by RT-PCR. B, Root length measurements of the lines described in A were assessed by ImageJ and are means of triplicate data sets ($n = 15$ per replicate). Error bars represent the mean ± SE. C, Basic fuchsin staining of the primary roots of 14-dpg seedlings of Col-0 and *lac2* mutants grown under control conditions for visualization of lignin captured at 10× magnification. Scale bar = 100 μm. D, Basic fuchsin-stained roots of the above-mentioned lines at 63× magnification captured from 10–12 cells above the initiation of the EZ. Scale bar = 10 μm. E, Visualization and comparison of cell wall-associated phenolics of the indicated lines by UV-induced autofluorescence. Px, Protoxylem; Mx, metaxylem. Scale bar = 20 μm. F, Integrated density was measured in arbitrary intensity units and the two lines were compared using ImageJ with five samples for each line. G, Comparison of total lignin content in roots of Col-0 and *lac2* mutants by the thioglycolic acid method. Lignin estimation was performed with triplicate biological samples ($n = 15$). Asterisks indicate values that are significantly different from their equivalent control as determined by Student's *t* test (*$P < 0.05$; **$P < 0.01$).

mutant, expression analysis of other *LACCASEs* was performed in the *lac2* mutant. Expression of any of the *LACCASE*s was not significantly altered in the mutant line compared to the wild type plant, at least at the transcriptional level (Supplemental Fig. S2B). 3,3-Diaminobenzidine (DAB)-staining and quantification did not show any significant difference in peroxidase activity between the Col-0 and *lac2* roots (Supplemental Fig. S2, C and D), suggesting that high constitutive lignin content in the root elongation/differentiation zone (EDZ) of the *lac2* mutant was directly related to *LAC2* expression. Restoration of *LAC2* expression by expressing *LAC2* cDNA under the 1.5-kb-long native promoter in the *lac2* background (*lac2*/P_{LAC2}::*LAC2*) rescued the short root phenotype of the mutant (Fig. 3A). Metaxylem differentiation and lignin deposition in the *lac2*/P_{LAC2}::*LAC2* line were similar to those in the Col-0 plants (Fig. 3E), suggesting that the higher root lignin and short root phenotype of the *lac2* mutant were due to the absence of *LAC2* expression. In addition to the *lac2*/P_{LAC2}::*LAC2* line, overexpression of *LAC2* using the *Cauliflower mosaic virus* (CaMV)35S promoter (LAC2OX) in Col-0 resulted in a small but significant increase in root length and a reduction in lignin content (Fig. 3, A–F). The *LACCASE2* gene showed expression only in the stele region of the root when a reporter gene, *CFP* (*cyan fluorescent protein*), was expressed under control of the *LAC2* promoter (Fig. 3G). All the results described above suggested a strong relation between the increased lignin deposition in root vascular tissues and the depletion in *LAC2* transcript abundance. Previously, the double mutants of *lac4* and *lac17* displayed a lower lignin content in the stem (Berthet et al., 2011) and the triple mutant *lac4lac11lac17* displayed almost complete depletion of lignin deposition in roots (Zhao et al., 2013), indicating that those genes acted as positive regulators of lignin deposition. In contrast, *lac2* mutant showed higher lignin deposition in root vascular tissues, particularly in xylem poles. Taken together, the results described here strongly suggest that *LAC2* acts as a negative regulator of xylem differentiation and lignification in roots.

LAC2 Is Posttranscriptionally Regulated during Water Deficit

To examine the regulation of *LAC2* expression, the plants expressing the *CFP* reporter gene under control of the *LAC2* promoter were subjected to 0.4 M mannitol treatment for 48 h Surprisingly, no significant change in *CFP* transcript level in roots was observed after mannitol treatment (Fig. 4A). Therefore, the possibility of a posttranscriptional regulation of *LAC2* expression was investigated. *LAC2*, *LAC4*, and *LAC17* mRNAs have been reported to be targets of *miRNA397* (Sunkar and Zhu, 2004). In Arabidopsis, the miR397 family is encoded by two genes, *miR397a* (At4g05105) and *miR397b* (At4g13555), that are physically separated by ~5 Mb on chromosome 4. The sequences of mature *miR397a* and *miR397b* differ by a single base at the seed region (Supplemental Fig. S3A). Expression analysis of these miRNAs in roots by stem-loop reverse-transcription quantitative PCR (RT-qPCR) using specific primers showed quick elevation of *miR397b* transcripts within 1 h of mannitol treatment, with a 4-fold increase after 48 h (Fig. 4B). On the other hand, the basal expression level of *miR397a* was distinctly very low in roots and did not show a significant change even after 48 h of mannitol treatment, which agrees with the previous finding based on sequence read count (Sunkar and Zhu, 2004). In Arabidopsis seedlings, *miR397b* was predominantly expressed in roots, with relatively lower expression in shoots, while *LAC2* showed an inverse expression profile with low and high expression levels in roots and shoots, respectively. Expression levels of *LAC4* and *LAC17* in roots and shoots were similar (Supplemental Fig. S3B, i and ii). Expression of *miR397b* in roots was analyzed by expressing a GUS reporter gene fused to the ~0.8 kb promoter of *miR397b*. Results showed that *miR397b* expression was highly elevated in the stele by mannitol treatment (Fig. 4C). RNA ligase-mediated RACE (RLM-RACE) followed by sequencing validated cleavage of *LAC2* mRNA at the predicted *miR397b* target site after the 690th nucleotide from the transcription initiation site (Supplemental Fig. S3C). Localization of *LAC2* and *miR397b* expression in the same tissue, inverse expression patterns, and validation of the predicted target mRNA cleavage site suggested that water deficit-mediated depletion of *LAC2* transcript level might be regulated posttranscriptionally by *miR397b*.

miR397b Regulates *LAC2* Expression and Root Lignification

To understand the role of *miR397b* in regulating *LAC2* expression and root lignification, a precursor molecule of the miRNA397b was expressed under the CaMV35S promoter in Col-0 (*miR397b*OX). Additionally, a short tandem target mimic (STTM) construct was synthesized as described previously (Yan et al., 2012) that had two copies of *miR397b*-binding oligonucleotides with three extra bases inserted between nucleotides 10 and 11 in the miR397b-target site to prevent target cleavage (Supplemental Fig. S4A). The construct was expressed under the CaMV35S promoter to block *miR397b* function in Col-0 plants. Expression of *miR397b* and *LAC2* in multiple transgenic lines was assessed (Supplemental Fig. S4A). Root length, xylem differentiation, and lignin deposition in xylem poles of the representative *miR397b*OX and STTM lines were compared with those in the Col-0 and *lac2* lines. *LAC2* expression in the roots of these plants was compared (Fig. 5A), and as expected, in the given experimental condition, *LAC2* expression was either not detectable or very low in the *lac2* and *miR397b*OX lines, while it was high in the STTM-harboring plants. Measurement of primary root length of 14-dpg plants and assessment of

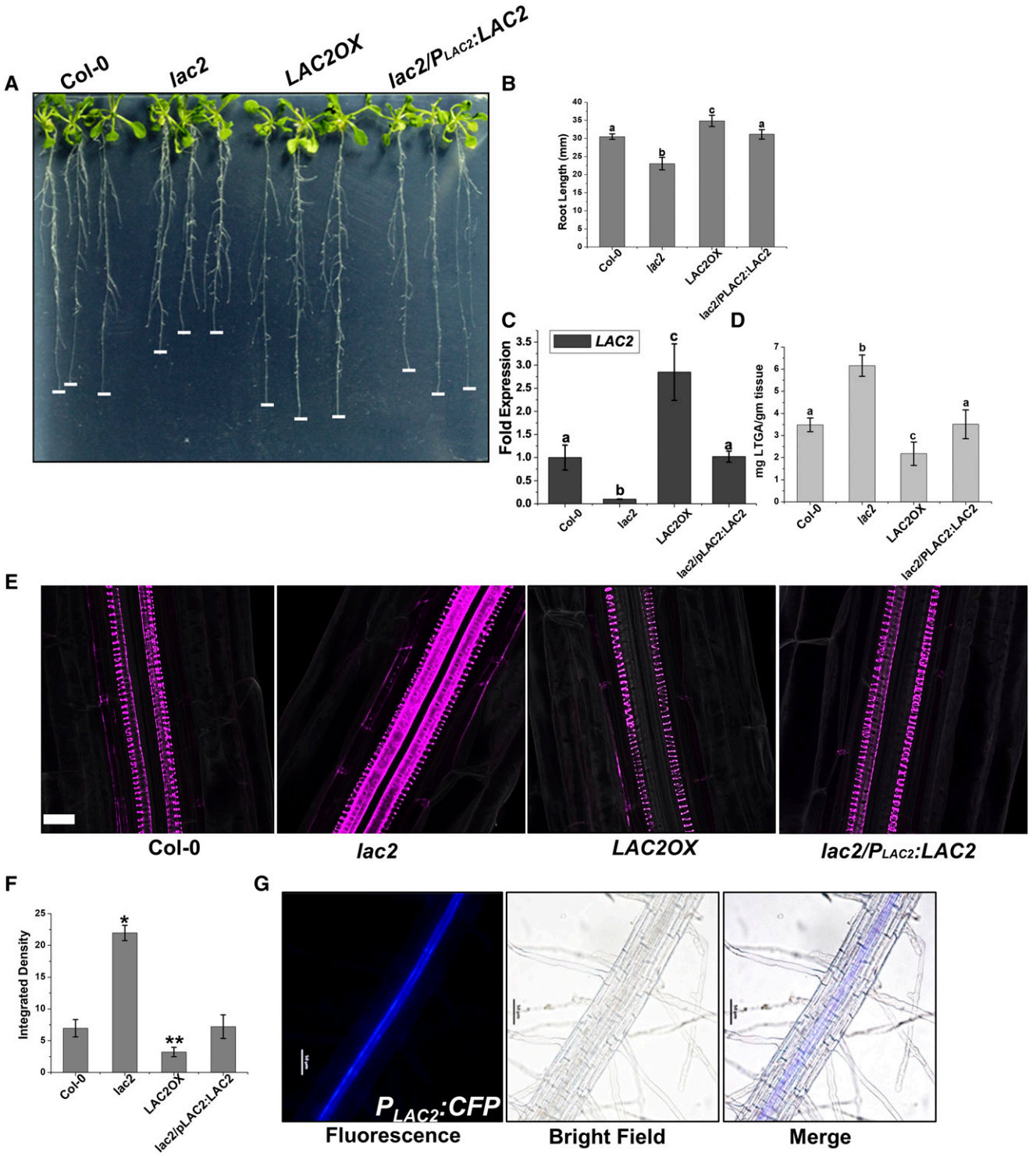

Figure 3. Root growth and lignin deposition are affected by *LAC2* expression. A and B, Primary root length phenotype (A) and measurement (B) of 14-dpg seedlings of Col-0 and the *lac2* mutant line were compared with *LAC2*-overexpressing (*LAC2OX*) and *lac2/*P_{LAC2}*::LAC2* complementation lines under normal growth conditions. Root length data are the means of three replicates (n = 15). Lowercase letters represent significant differences among the values under study ($P < 0.05$) as determined by one-way ANOVA. Error bars represent the mean ± SE. C, Fold expression of *LAC2* in the mutant and transgenic lines relative to that in Col-0 was determined by RT-qPCR. *AtACTIN2* was used for normalization. Error bars represent the mean ± SE. D, Total root lignin content estimation of the Arabidopsis lines mentioned above using the thioglycolic acid method. E, Basic fuchsin staining of 14-dpg roots of the plant lines mentioned above. The images, taken at 63× magnification, were captured from 10–12 cells above the

xylem pole lignification by staining and root lignin content estimation clearly showed that the plants with high *LAC2* expression displayed reduced root metaxylem differentiation and lignification and increased root length (Fig. 5, B–E). These results demonstrated the regulatory role of *miR397b* in *LAC2* expression and metaxylem differentiation in roots. To further substantiate this result, a modified *LAC2* cDNA (*rLAC2*) with two nucleotides altered at the *miR397b*-target site was expressed under the *LAC2* promoter in the *lac2* mutant. The representative *lac2* line expressing *rLAC2* exhibited a high *LAC2* transcript level, very low root lignification in metaxylem poles, and increased root length in normal growth conditions (Fig. 5, A–E; Supplemental Fig. S4B). Expression of *LAC4* and *LAC17*, the other targets of *miR397b*, was assessed in roots of two independent *miR397b*OX lines. *LAC17* expression did not show significant alteration, while the *LAC4* transcript level was reduced by a maximum of 1.3-fold. Notably, *LAC2* expression in root was reduced by ~7–fold, indicating that *LAC2* mRNA is the major target of *miR397b* in roots (Fig. 5F). To explore the epistatic relationship between *miR397b* and *LAC2*, *miR397OX* and *rLAC2* lines were crossed to have a *miROXrLAC2* line. The root length and root lignin content of the *miROXrLAC2* line were similar to those of the *rLAC2* line, suggesting that miR397b is genetically epistatic to LAC2 (Supplemental Fig. S5).

All the transgenic lines described above were subjected to 0.4 M mannitol treatment at 4 dpg for an additional 8 d, and fold reduction in primary root growth was measured on alternate days. Increase in root lengths of the plant lines with high *LAC2* expression (*LAC2*OX, STTM, and r*LAC2*) under mannitol treatment was ~0.4-fold of their increase under normal growth conditions after 8 d of treatment, whereas increase in root lengths of *lac2* and *miR397b*OX, with low *LAC2* expression, was only ~0.15-fold of their increase under normal conditions. Root lignin content in these lines showed an inverse relation to the root length increase (Fig. 6, A and B). Basic fuchsin staining after 48 h of mannitol treatment showed early differentiation of root xylems, as evident by lignin deposition in the xylem poles. Lignin deposition was more intense and closer to the root tip in the case of the *lac2* mutant. However, lignin deposition was comparatively less in *LAC2OX*, STTM, and *rLAC2* lines than in the wild-type plants (Fig. 6C). These results emphasized that *miR397b* regulates *LAC2* expression and lignification in root vascular tissue under water deficit condition. Root growth arrest in the presence of mannitol depends on multiple factors in addition to lignin deposition. Lignin deposition and root growth arrest even in the plants with high *LAC2* expression were distinctly higher under mannitol treatment compared to normal growth conditions, suggesting that the LAC2-mediated pathway is partly responsible for root vasculature lignification and root growth inhibition during water deficit.

miR397b-LAC2 Module Enhances Lignin Deposition in Root EZ under Pi Deficiency

Plants respond to suboptimal Pi with primary root growth arrest associated with a sharp decrease in cell proliferation and elongation in the root meristem and EZ associated with high lignin deposition in the EZ (Müller et al., 2015; Balzergue et al., 2017). A mutant plant (*lpr1lpr2*) with reduced sensitivity to low Pi-associated root growth inhibition displayed much lower lignification at the EZ compared to the mutant with high sensitivity to low Pi (*pdr2*; Müller et al., 2015; Ziegler et al., 2016). To determine whether LAC2-dependent lignification is specific to water deficit stress or has a role in other abiotic stresses, such as phosphate deprivation, 3-dpg Col-0 and *lac2* plants grown in a medium containing 625 μM Pi were transferred to different low-Pi (60, 40, and 0 μM Pi) media for 48 h. Both Col-0 and *lac2* plants showed reduced root growth rate, but *lac2* plants were hypersensitive to low Pi conditions (Fig. 7A; Supplemental Fig. S6A) with higher lignin deposition at the root EZ (Fig. 7B). Relative fold expression of all the *LACCASE* genes in various low-Pi media as compared to that in Pi-sufficient (625 μM; +Pi) medium showed reduced expression of *LAC2* and *LAC4* under low Pi (Supplemental Fig. S6B). To examine the role of the *miR397b-LAC2* module in root lignin deposition during Pi deprivation (−Pi), expression profiling of *miR397b* and its target transcripts *LAC2*, *LAC4*, and *LAC17* were analyzed by RT-qPCR in Col-0 roots grown in different suboptimal Pi conditions for 48 h as mentioned above. Expression of *LAC2* and *LAC4* in roots declined by ~9-fold and ~3-fold, respectively, upon transfer to −Pi (0 μM) medium. Expression of *LAC17* did not alter significantly by low-Pi treatment. On the other hand, *miR397b* expression was increased by ~6-fold in 60 μM Pi, and ~30-fold in −Pi medium (Fig. 7C). As observed in the case of the mannitol treatment, expression level of *CFP* under the *LAC2* promoter did not change significantly under Pi starvation (Fig. 7D), suggesting posttranscriptional regulation of *LAC2* during Pi deficiency. Three-day-old seedlings of *miR397b*OX, *LAC2*OX, and STTM lines were transferred from +Pi (625 μM) to −Pi (0 μM) media

Figure 3. (*Continued.*)
initiation of the EZ. Scale bar = 10 μm. F, Estimation of the integrated density of all lines under comparison, expressed in arbitrary units in the *y* axis. All estimations were done with five samples for each line. Asterisks indicate values that are significantly different from their equivalent control as determined by Student's *t* test (*$P < 0.05$; **$P < 0.01$). G, *LAC2* promoter activity in roots as determined by expression of the *CFP* gene driven under the *LAC2* promoter. Images are 20× magnifications captured from 10–15 cells above the initiation of the EZ. Scale bar = 50 μm.

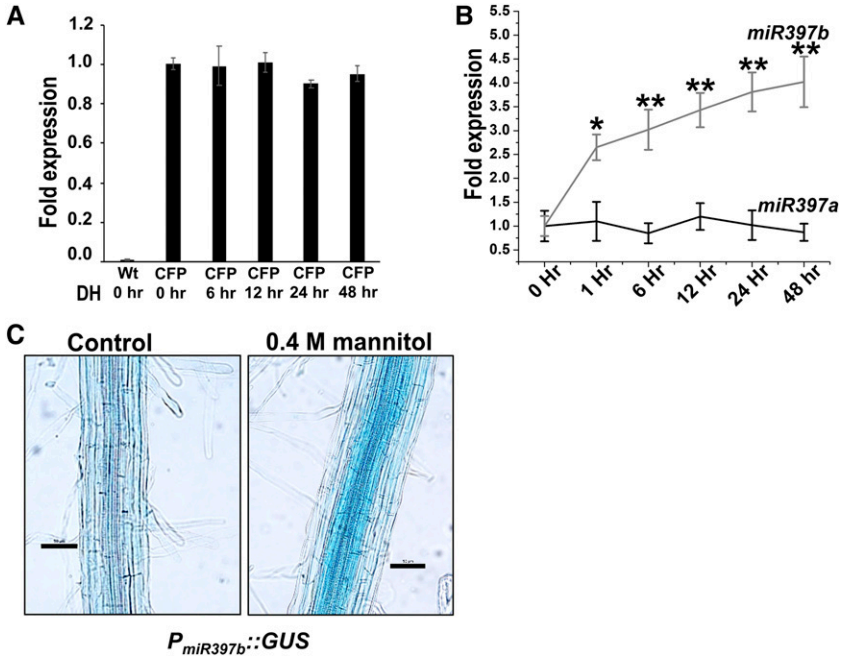

Figure 4. Expression analysis of *LAC2* and *miR397b* under water deficit. A, Expression of the *CFP* gene analyzed by RT-qPCR in roots of plants harboring P_{LAC2}*::CFP* and treated (DH) with 0.4 M mannitol for different time periods. Fold expression of *CFP* in response to mannitol treatment relative to that without treatment (0 h) was presented. The Col-0 (Wt) sample without treatment was used as a negative control. Error bars represent the mean ± SE. B, Fold expression analysis by stem-loop RT-qPCR of mature *miR397a* and *miR397b* in response to treatment with 0.4 M mannitol for different time periods. Fold expression under mannitol treatment was determined relative to that without treatment. Asterisks indicate values that are significantly different from their equivalent control as determined by Student's *t* test (*$P < 0.05$; **$P < 0.01$). C, Determination of in planta *miR397b* promoter activity by transferring 4-dpg Arabidopsis seedlings harboring the $P_{miR397b}$*::GUS* construct to media without (Control) or with 0.4 M mannitol for 48 h and staining with X-Gluc for *GUS* expression. The image was captured from 10–15 cells above the initiation of the EZ of both the seedlings at 20× magnification. Scale bar = 50 μm.

along with the Col-0 and *lac2* plants for 8 d and fold increase in primary root length was measured on alternate days. Although root growth was arrested in all the lines in −Pi media within 48 h, root growth retardation was comparatively more in the lines with lower *LAC2* expression (*lac2* and *miR397b*OX) than in the lines with higher *LAC2* expression (LAC2OX and STTM). STTM and *LAC2*OX lines also displayed comparatively much less lignin deposition in the EZ at 48 h after treatment (Fig. 8, A–C). However, the residual lignin deposition in these lines suggests the existence of LAC2-independent pathways of lignin accumulation in root EZ under Pi deficiency.

Low-Pi-mediated root growth arrest is modulated by iron (Fe^{3+}) availability in the medium and is associated with localized iron accumulation in the apoplastic region in the root apex (Svistoonoff et al., 2007; Ward et al., 2008; Müller et al., 2015). Localized iron accumulation was much higher in the *lac2* root EZ than in Col-0 roots under the Pi-deprived condition (Fig. 8D). To determine any role of miR397b and LAC2 in this physiological response, 3-dpg *miR397b*OX, *LAC2*OX, and STTM lines were transferred to –Pi medium for 48 h. *miR397b*OX lines showed a higher iron accumulation in the root EZ compared to the *LAC2*OX and STTM lines (Fig. 8D). Accumulation of iron in the root EZ was proposed to trigger production of reactive oxygen species, leading to callose deposition in the EZ and stem cell niche, resulting in meristem exhaustion (Müller et al., 2015; Balzergue et al., 2017). Callose deposition levels in the EZ and root apex in all the lines mirrored the iron accumulation in those lines upon exposure to –Pi medium, suggesting that there are direct relations between lignin deposition, iron accumulation, and callose deposition in the root EZ during Pi starvation (Fig. 8E). Overall, our result suggests a distinct and direct role of the miR397b-LAC2 module in this Pi-deficiency-mediated root growth arrest and the associated physiological response.

DISCUSSION

Root system architecture determines plant growth and productivity under water and nutrient stress. Small xylem diameter in the deep roots improves root hydraulic conductivity (Zimmermann, 1983; Tyree et al., 1994). An adaptive root system architecture with a strong, narrow, and less leaky xylem during water limitation has been predicted to hold promise for

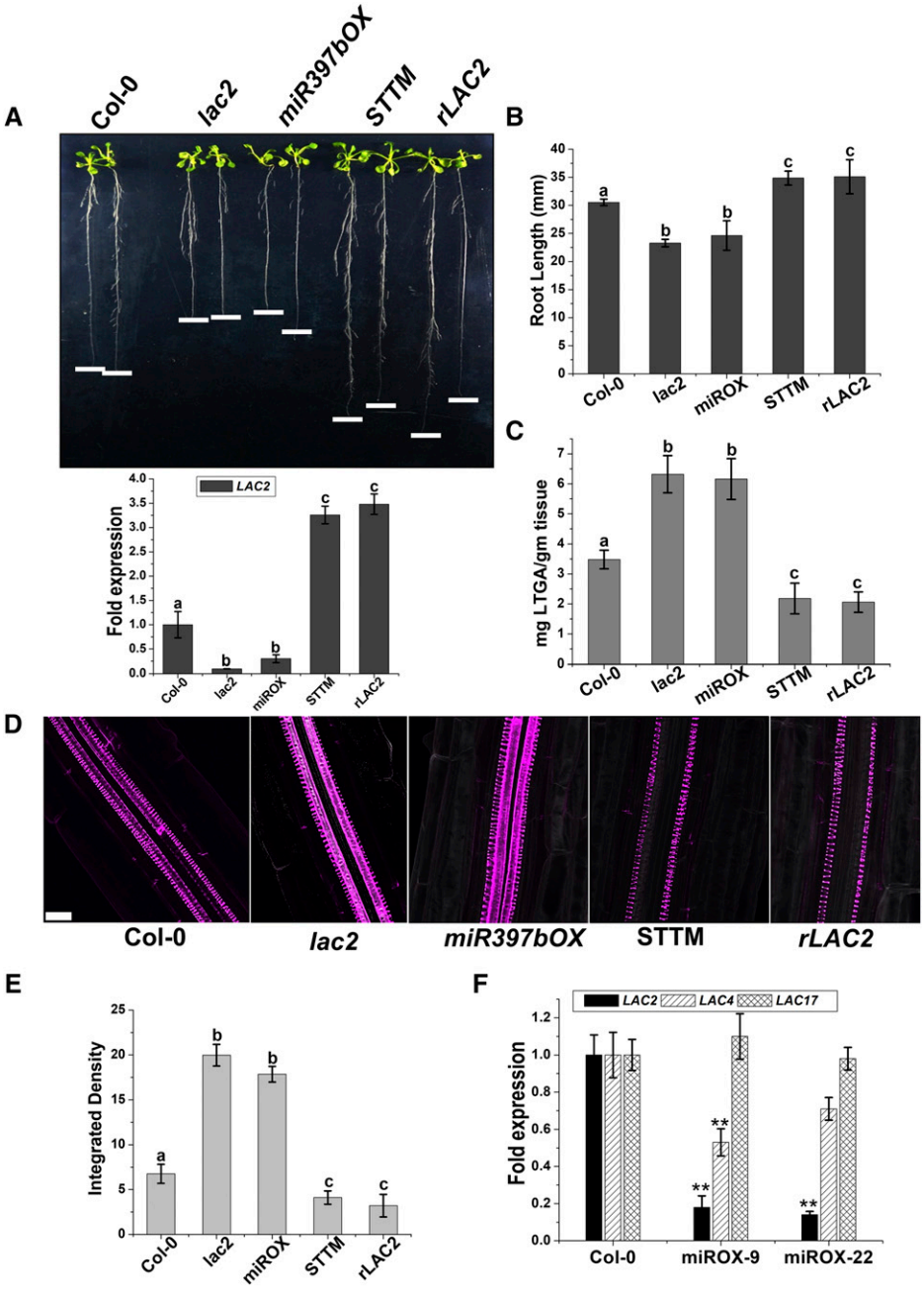

Figure 5. Comparison of root length and lignin deposition in Arabidopsis lines with enhanced and suppressed expression of *miR397b*. A and B, Comparison of primary root phenotype and length. Root length data are a representation of three replicates ($n = 15$). Lowercase letters represent significant differences among the values under study ($P \leq 0.05$) as determined by one-way ANOVA. Error bars represent the mean ± SE. The bars in A shows fold expression of *LAC2* in the indicated lines relative to that in Col-0 as assessed by RT-qPCR. *AtACT2* was used as internal control. C and D, Estimation of root lignin by thioglycolic acid (C) and visualization of lignin by basic fuchsin staining (D) in 14-dpg roots of the indicated lines. Images at 63× magnification were captured from 10–12 cells above the initiation of the EZ. Scale bar = 10 μm. E, Comparison of the integrated stain density using ImageJ with five samples for each line. Lowercase letters indicate significant differences among the lines under study. F, Expression analysis of *LAC2*, *LAC4*, and *LAC17* by RT-qPCR in two independent *miR397bOX* lines. Data from three biological replicates are presented. Asterisks indicate values that are significantly different from their equivalent control as determined by Student's *t* test (*$P < 0.05$; **$P < 0.01$).

improving plant productivity in intermittent drought conditions (Comas et al., 2013; Vadez, 2014). Water deficit-mediated growth arrest in the maize root EZ was accompanied by lignin deposition and narrowing of xylem vessels (Fan et al., 2006). A typical value of water potential that a plant cell experiences when it is exposed to "low water potential stress" is −1.0 MPa, while an unstressed cell experiences −0.2 MPa (Verslues et al., 2006). In this study, we have chosen 0.4 M mannitol that generates −1.0 MPa water potential (Takeba and Matsubara, 1979), which was within the natural range of osmotic stress. Intense lignification in the wheat and rice root vasculature was associated with drought and salinity tolerance (Jbir et al., 2001; Lee et al., 2016). Lignin deposition in the root vascular tissue shows an adaptive plant response to support water and nutrient transport through root in adverse environmental conditions. In this report, we have proposed enhancement of the localized lignin deposition in root xylem poles as a plant developmental response mechanism during water and nutrient stresses.

Role of LAC2 in Root Lignification

PEROXIDASEs and LACCASEs are known to oxidize lignin precursors at the plant cell walls. Catalytically, they use different forms of oxygen for their activities. It was shown through a genome-wide

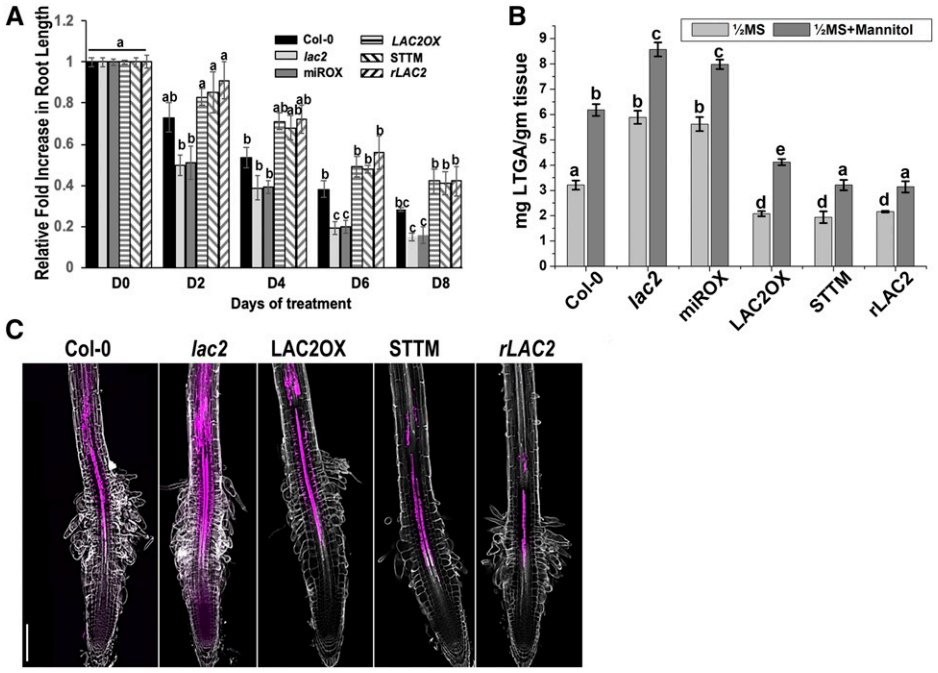

Figure 6. Comparison of fold changes in root length and lignin content in transgenic Arabidopsis lines under water deficit. A, Comparison of the relative fold increase in root length of Col-0, *lac2*, and transgenic Arabidopsis lines upon treatment of 4-dpg seedlings with 0.4 M mannitol for various periods up to 8 d (D0–D8). The increase in root length under mannitol treatment relative to that in the untreated condition for the same period is presented as the relative fold increase in root length for each line. Values represent data from three replicates ($n = 15$). Error bars represent the mean ± SE. B, Quantification of lignin in roots of transgenic plants at the end of treatment in both growth conditions by the thioglycolic acid method. Lowercase letters in A and B represent significant differences among the values under study ($P < 0.05$) according to two-way ANOVA. C, Roots of 4-dpg seedlings of the mentioned plant lines were treated with 0.4 M mannitol for 48 h and stained with basic fuchsin and calcofluor white after the treatment for visualization of lignin at 20× magnification. Scale bar = 50 μm.

transcriptome analysis that the functions of LAC4, LAC11, and LAC17 were most probably nonredundant with PEROXIDASEs (Zhao et al., 2013). We did not observe any significant change in peroxidase activity in the root of the *lac2* mutant. Conversely, peroxidase-mediated polymerization of lignin that augments Casparian strip formation appeared to be LACCASE independent, as it was shown to be dependent on hydrogen peroxide (H_2O_2) production (Lee et al., 2013). Therefore, it appears that functions of at least some of the LACCASEs are nonredundant with PEROXIDASEs. As described before, there is very little evidence regarding the direct role of plant LACCASEs in lignification of the cell wall. The absence of distinctly visible phenotypic differences in most of the single *lac* mutants in normal growth conditions indicates redundant or cooperative functions of these family members (Cai et al., 2006). Therefore, significantly visible high root lignin deposition due to the absence of only *LACCASE2* was intriguing. At present, we do not envisage any role of LAC2 in lignin depolymerization. It might have a role in inhibiting the activity of other prolignifying LACCASEs or in reducing the production of monolignol radicals by other LACCASEs/PEROXIDASEs that would explain the high root lignin deposition in the *lac2* mutant. Therefore, in natural stress conditions, functions of other LACCASEs/PEROXIDASEs are also vital for root lignin deposition. Root xylem development shows morphological plasticity in response to environmental changes such as water limitation. Phytohormone ABA is necessary for proper root xylem development. Plants defective in ABA biosynthesis or signaling displayed xylem strands that were discontinuous or absent. An elevated ABA level induced formation of an extra xylem strand. It has been proposed that an elevated level of miR165 and its target HD-ZIP III, a transcription factor, may play a role in regulating root xylem morphology (Ramachandran et al., 2018; Bloch et al., 2019). Our results showed similar intense proto- and metaxylem differentiation following mannitol treatment. However, the roles of miR397b and its target, *LAC2*, were more evident in the case of metaxylem differentiation. The role of ABA in regulation of miR397b expression would be worthy of investigation.

Role of LAC2 in Root Growth

We have used two *lac2* mutant (SALK_025690C and SAIL_292_B04) to substantiate our observation that LAC2 has a role in root xylem differentiation and xylem pole lignification. Compromised root elongation of the

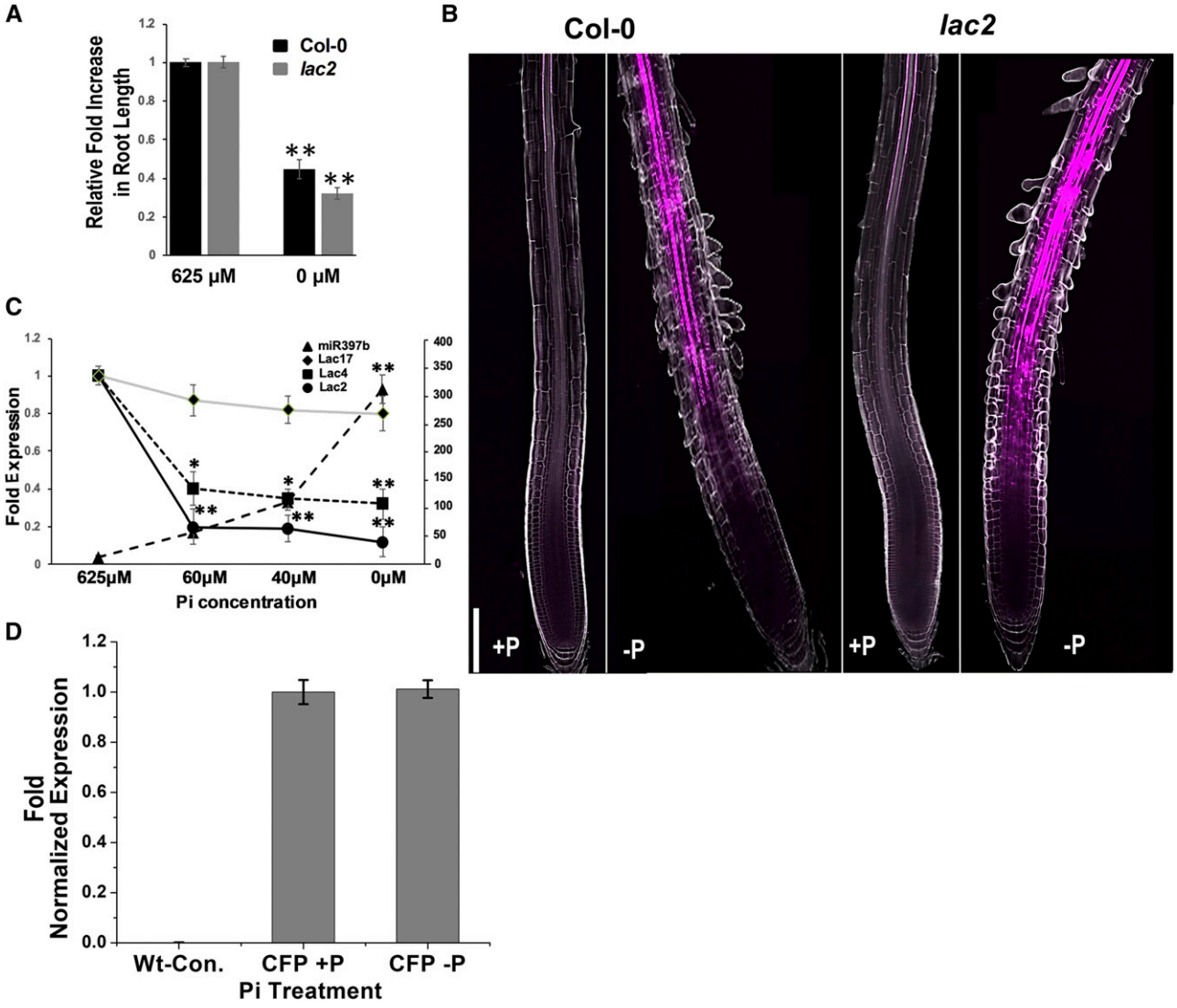

Figure 7. Root growth arrest and lignin deposition under low Pi in Col-0 and *lac2* plants. A and B, Comparison of primary root length (A) and lignin deposition (B) by staining after plants were transferred to sufficient (625 μM) and deficient (0 μM) Pi medium for 48 h. Increase in root length in Pi-deficient medium relative to that in Pi-sufficient medium is presented as the relative fold increase in root length. Root lengths represent data from three biological experiments ($n = 15$). Error bars represent the mean ± SE. C, Expression analysis of *LAC2*, *LAC4*, and *LAC17* by RT-qPCR and of *miR397b* by stem-loop RT-qPCR after treatment under Pi-sufficient and Pi-deficient conditions for 48 h The primary and secondary *y* axes represent fold expressions of target genes and *miR397b*, respectively, at various Pi-deficient media relative to that in Pi-sufficient (625 μM) medium. D, Comparison of *LAC2* promoter activities as determined by *CFP* expression under its control in 3-dpg plants harboring P_{LAC2}::*CFP* (*CFP*) after growing in Pi-sufficient (+P) and Pi-deficient (−P) media for 48 h. Fold expression of *CFP* in −Pi medium relative to that in +Pi medium is presented. *CFP* expression in Col-0 plants (Wt-Con.) was used as a negative control. Asterisks indicate values that are significantly different from their equivalent control as determined by Student's *t* test (*$P < 0.05$; **$P < 0.01$).

SALK mutant line under polyethylene glycol treatment was reported before (Cai et al., 2006). Developmental defects have been reported in lignin-deficient plants such as *lac4lac17* and *lac4lac11lac17* mutants. While *lac4lac17* showed a dwarf shoot phenotype under continuous light, *lac4-2lac11lac17* had severely stunted shoots and narrower roots with no visible lignification under the normal long-day growth condition (Berthet et al., 2011; Zhao et al., 2013). Previously, two CCR1-deficient mutants were shown to display lignin deficiency and dwarf phenotype (Mir Derikvand et al., 2008). Interestingly, the decrease in root growth rate of the *lac2* mutant began at 6 dpg and continued. It would be noteworthy to mention that the root apical meristem (RAM) reaches its final size at 5 dpg, and then cell elongation and differentiation initiate to define the final root length (Moubayidin et al., 2010). *LAC2* promoter activity was not detected in the RAM even in the

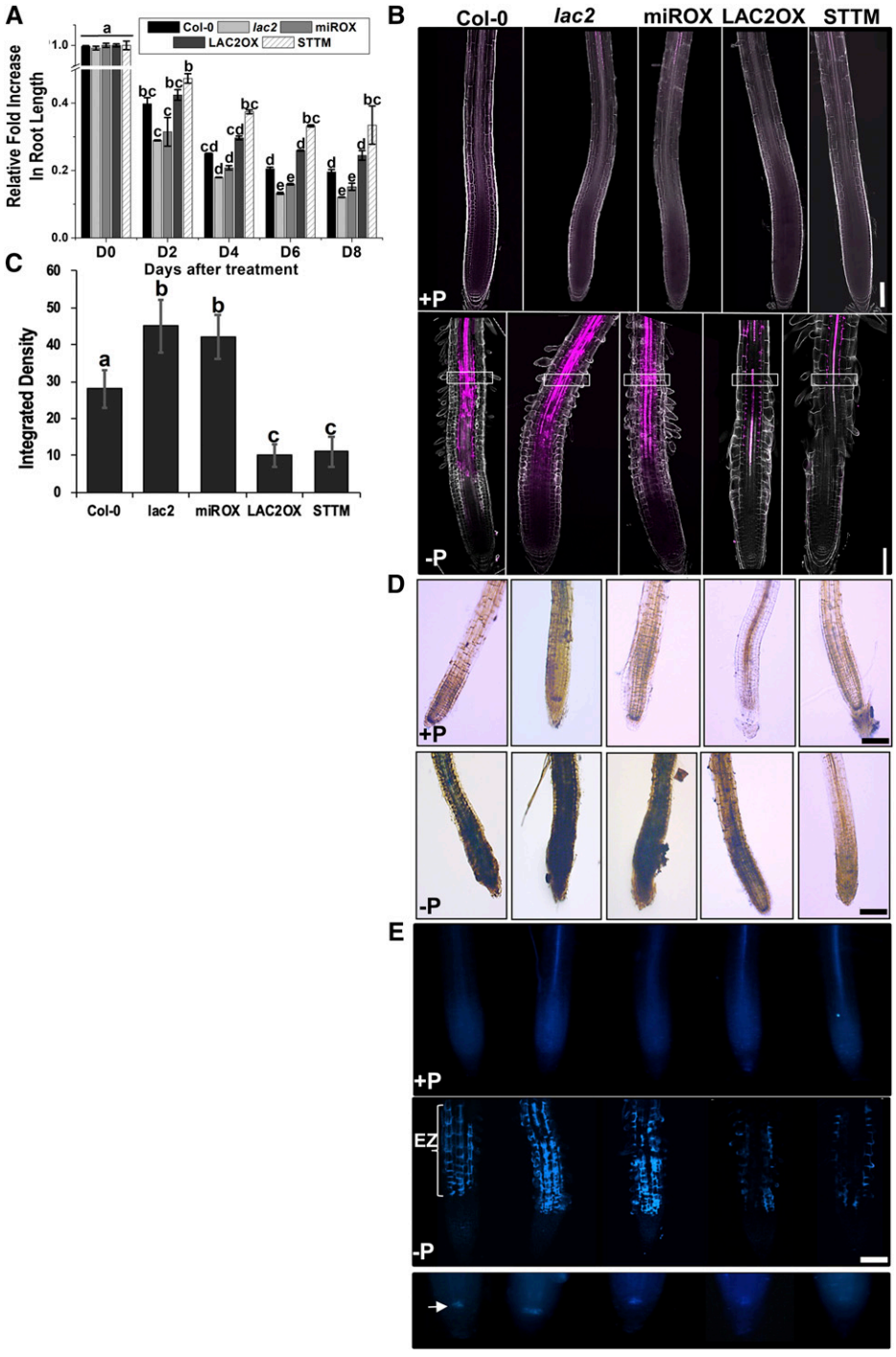

Figure 8. Root length and deposition of lignin, iron, and callose in the root EZ of Arabidopsis lines with enhanced and suppressed expression of *LAC2* under low Pi condition. A, Seedlings of the Arabidopsis lines mentioned were transferred to Pi-sufficient (+P; 625 μM) and Pi-deficient (−P; 0 μM) media for 8 d (D0–D8), and the increase in root length was compared. Increase in root length in −P medium relative to that in +Pi medium is presented as the relative fold increase in root length. Data represent values for three replicates (n = 15). Lowercase letters represent significant differences among the values under study ($P < 0.05$) according to two-way ANOVA. Error bars represent the mean ± SE. B, Basic fuchsin staining shows accumulation of lignin in the root EZ under +P and −P treatments for 48 h. Scale bar = 50 μm. Rectangular boxes indicate the regions taken for comparison of integrated density measurements. C, Comparison of integrated density of fuchsin stain in the boxed areas in C. Integrated density was measured using ImageJ with five samples for each line. Lowercase letters represent significant differences among the values under study ($P < 0.05$) according to one-way ANOVA. D, Perl's/DAB iron staining shows iron deposition in the root EZ of different lines under +P and –P treatments for 48 h, as mentioned in B. Scale bar = 100 μm. E, Aniline blue staining for callose deposition in the root EZ and stem cell niche (arrow in the lower image) of Arabidopsis lines mentioned in B after 48 h of +P and −P treatments. Scale bar = 50 μm.

mature plant, and lignification in *lac2* mutant roots was not detected before 5 dpg (Supplemental Fig. S7), suggesting that LAC2 is most probably active only in the differentiated vascular tissues in the Arabidopsis root under the normal growth condition. It was already demonstrated with maize (*Zea mayz*) root that water deficit-mediated lignification of the root vascular tissue is involved in progressive inhibition of cell wall extensibility (Fan et al., 2006). All of these observations suggested that the short root phenotype of these mutant lines was due to higher lignin deposition in the root vascular tissue. Inhibition of root growth and lignin deposition in the EZ were observed in the case of a mutated gene encoding the plasma-membrane-bound receptor-like kinase *THESEUS1* in the *cesa6* mutant background, which is defective in cellulose synthesis, and therefore, *THESEUS1* is considered a sensor of cell wall perturbation (Hematy et al., 2007; Merz et al., 2017). At this point, the status of cellulose synthesis and content in the *lac2* mutant and the functional

relationship between *THESEUS1* and *LAC2* in the context of primary cell wall biosynthesis or degradation are not clear.

Role of LAC2 in Water and Nutrient Deficiency

Root growth arrest and lignin deposition in the root vascular tissues in response to stress may be interdependent processes. Lignin is generally deposited in the secondary cell walls of differentiated cells, and root growth is primarily determined by the dividing cells at the RAM and, additionally, by elongation of differentiated cells. Excess lignin deposition reduces the xylem vessel diameter, limiting water and nutrient transport (Fan et al., 2006). Additionally, lignin deposition also restricts extensibility of the xylem and endodermal cells. Elongation of other cells in the root differentiation zone might be synergistic with xylem cell elongation. A situation of restricted water and nutrient transport might be sensed by the RAM and other differentiated cells affecting reduced cell division and elongation. Relatively shorter root length of the mutant/transgenic plants with low *LAC2* expression under the normal growth condition can be explained by relatively higher lignin deposition, decreased water and nutrient transport, and their effects on cell elongation and division. Root length was similar in wild-type and *lac2* plants until the appearance of lignified root vascular tissue, suggesting a connection between lignin deposition and root growth arrest. RAM size was smaller in the *lac2* plant than in the wild-type plants. However, in the water-limiting condition, root growth arrest precedes lignin deposition, and we believe that lignin deposition causes an additional negative effect on root growth by reducing water and nutrient transport and cell wall extensibility. We have also observed lignin deposition in the endodermal cell layer in the elongation/differentiation zone within 48 h after mannitol treatment.

Conversely, Pi-deficiency-mediated root growth arrest seems to follow a different pathway. It was shown that only physical contact of the root tip with the low-Pi medium is necessary for growth arrest (Svistoonoff et al., 2007). A significant decline in the number of dividing and elongating cells in the RAM was observed within a short period of low-Pi exposure, suggesting a shift from cell division to differentiation mode (Müller et al., 2015). This was followed by lignin deposition in the EZ (Ziegler et al., 2016), possibly negatively affecting cell elongation. The loss-of-function mutant of two multicopper oxidase genes, *lpr1lpr2*, showed reduced root growth arrest and reduced lignin deposition in the EZ in low-Pi medium. Similarly, plants with high *LAC2* expression displayed decreased lignin deposition in this zone and reduced root growth arrest compared to the plants with low or no expression of *LAC2*. As the *LAC2* transcript level is regulated by miR397b, genetic interaction between LPR and miR397b needs to be worked out to define part of the low-Pi-mediated root growth arrest pathway. It was reported before that the presence of external Fe was necessary for low-Pi-induced growth arrest (Svistoonoff et al., 2007; Müller et al., 2015). We observed high local accumulation of lignin and Fe in the *lac2* mutant and the *miR397b*OX line. Further, lignin deposition in the EZ was not observed in the absence of Pi and Fe (Supplemental Fig. S8), which suggests that there is cross talk between Fe and lignification during Pi starvation. In this study, we have provided a mechanism by which the *miRNA397b-LAC2* module deposits lignin in the root EZ under the low-Pi condition. We hypothesize that high lignin deposition in root EZ due to miR397b-mediated reduced *LAC2* expression led to the formation of a stiff and hydrophobic secondary cell wall and increased localized Fe and callose deposition exerting a double negative impact on root growth under Pi deficiency. Root growth arrest under low Pi involves multiple genetically uncoupled mechanisms leading to inhibition of cell proliferation and elongation (Singh et al., 2014; Balzergue et al., 2017; Gutiérrez-Alanís et al., 2017), and some of those mechanisms might be responsible for root growth arrest in low Pi even in the absence of lignin deposition in the root EZ in plant lines with high *LAC2* expression.

Regulation of *LAC2* Expression in Roots

Involvement of LACCASEs in stress response could be envisaged from the altered expression patterns of the *LACCASE* genes in adverse conditions. In a previous study, *LAC2* expression was shown to be down-regulated by ≥4-fold in roots in response to all the abiotic stress treatments tested (Toufighi et al., 2005). Our results also showed significant down-regulation of *LAC2* expression in roots in response to mannitol and low-Pi treatment. Among the three targets of *miR397b*, *LAC2*, *LAC4*, and *LAC17*, transcriptional control of *LAC2* was reported to be different from that of the two other targets. As a part of the secondary cell wall biosynthesis program, these *LACCASE* genes were thought to be under the control of the NAC SECONDARY CELL WALL THICKENING PROMOTING FACTOR (NST) transcription factor family (Mitsuda et al., 2005, 2007). *LAC4* and *LAC17* expression was significantly down-regulated in the *nst1nst2nst3* triple mutant, whereas these genes appeared to have no effect on *LAC2* expression (Zhao et al., 2013). Our result indicated that the *LAC2* transcript level in roots was predominantly regulated by a posttranscriptional mechanism even in normal growth condition. Its expression level was inversely proportional to that of *miR397b*. Additionally, *LAC2* promoter activity did not change in any of the stress conditions tested in this study, and expression of the STTM construct increased the steady-state expression level of *LAC2* in the normal growth condition. *Arabidopsis miR397b* was shown to target *LAC4* in the stem (Wang et al., 2014), and *miR397a* was shown to be a negative regulator of expression of many of the *LACCASE*s in Poplar

(*P. trichocarpa*; Lu et al., 2013). Both previous results and those presented here showed a very low level of *miR397a* expression compared to a high level of *miR397b* expression in roots in normal growth conditions and in response to abiotic stress treatments in Arabidopsis (Sunkar and Zhu, 2004). It appears that *miR397* family members have different functions in different species and in different tissues. On examination, we did not find a preponderance of abiotic-stress-responsive cis-acting elements in the promoter sequence; of *miR397b*; rather, many potential development-associated cis-acting elements were located there (not shown). Therefore, it seems that *miR397b* responds to many of the abiotic stresses as a common response, and that expression of *miR397b*, and consequently of *LAC2*, in roots is regulated by stress response-mediated developmental cues.

We have presented a study describing a mechanism for the regulation of lignin deposition in root xylem poles and the EZ under water- and phosphate-deficient conditions, respectively, by the *miR397b-LAC2*-mediated pathway. Our results showed that LAC2 is a negative regulator of lignin deposition in these root tissues. Biosynthesis of monolignol from phenyl Ala occurs in multiple steps and involves several enzymes. Therefore, regulation of monolignol synthesis and lignin deposition would require fine-tuning of many rate-limiting steps. Modulating lignin deposition by using a negative regulator involved in the final step of lignin formation might be an additional and quick control for plant growth and development.

MATERIALS AND METHODS

Plant Material, Growth Conditions, and Stress Treatments

Seeds of wild-type Arabidopsis (*Arabidopsis thaliana*), ecotype Col-0, and *LACCASE2* T-DNA insertion lines (SALK_025690C and SAIL_292_B04) were procured from the Arabidopsis Biological Research Center (The Ohio State University, Columbus). Primers specific for T-DNA borders were used to screen homozygous lines of SALK_025690C and SAIL_292_B04. For all treatments, seeds were surface sterilized and grown on one-half strength Murashige and Skoog (MS) medium containing 1% (w/v) Suc (Sigma-Aldrich) and 0.8% (w/v) agar (Duchefa Biochemie) in a growth chamber under a 16 h light/8 h dark photoperiod at 21°C to 23°C unless otherwise indicated.

For mannitol (0.4 M) treatment, plants were vertically grown for 4 d and subsequently transferred onto one-half strength MS medium containing mannitiol and allowed to grow in a growth chamber for the indicated time periods (Figs. 1, 4, and 6). Root length was marked each day after treatments. Low-Pi and Fe-deficient media were prepared as previously described by Singh et al. (2014, 2018). Seedlings were grown on one-half strength MS medium for 3 d and subsequently transferred onto +Pi (625 μM) and Pi-deficient (60, 40, and 0 μM) media for the indicated time periods and root growth was measured each day using ImageJ software (Figs. 7 and 8; Schneider et al., 2012).

Construct Preparation and Transformation in Arabidopsis

For constitutive and promoter fusion expression constructs of LAC2 and miRNA397b, Gateway binary cloning technology (Invitrogen) was used according to the instruction manual. For constitutive expression, both LAC2 and miRNA397b were cloned in the pGWB2 vector under the CaMV35S promoter. The STTM construct for miRNA knock-down lines was designed as described by Yan et al. (2012) using primers listed in Supplemental Table S1. Complementation and cleavage-resistant LAC2 lines were generated by transforming the *lac2* T-DNA mutant in the pBI101.2 vector harboring the complete *LAC2* cDNA coding sequence and a modified *LAC2* coding sequence with mutated nucleotides at its cleavage site, respectively, under its own promoter. Plants were transformed by the *Agrobacterium tumefaciens*-mediated floral dip transformation method, as previously described by Clough and Bent (1998), and the transformants were selected on appropriate antibiotics.

RNA Extraction and Expression Analysis

Total RNA was extracted using TRI reagent (Sigma-Aldrich) and first-strand cDNAs were synthesized using SuperScript III Reverse Transcriptase (Thermo Fisher Scientific) according to the manufacturer's protocol. Expression analysis of miRNA and its respective target genes was performed by RT-qPCR using a ViiA7 Real-Time PCR System (Applied Biosystems) with three biological replicates. For miRNAs, stem-loop primers were designed and cDNA for individual miRNAs was prepared by pulsed-RT reaction using SuperScript III Reverse Transcriptase as described previously (Chen et al., 2005; Varkonyi-Gasic et al., 2007). Relative expression of genes was calculated according to the $\Delta\Delta$ C_t method (Livak and Schmittgen, 2001) and normalized with the *AtACTIN2* gene (At3g18780). Fold expression values from RT-qPCR were represented in heat maps using TIGR Multi Experiment Viewer (version 4.9).

Northern blot analysis of miRNA was performed as described previously (Lu et al., 2007; Rosas-Cárdenas et al., 2011). In brief, small RNAs were enriched by treating total RNA with PEG and NaCl, followed by 3 M sodium acetate precipitation. Then, 15 μg of enriched small RNAs was separated on denaturing (7 M urea) 15% polyacrylamide gel and transferred to a Hybond-N+ membrane (Amersham Biosciences). Antisense oligo for miRNA397b was synthesized and a probe was prepared by end labeling of oligo with γ-ATP using polynucleotide kinase enzyme (New England Biolabs). AtU6 RNA was used as an internal control. The primers used in this study are provided in Supplemental Table S1. *AtACT2* was used as an internal control.

RNA Ligase-Mediated RACE

Validation of miRNA-mediated cleavage of target mRNA was performed by RLM-RACE as described by Llave et al. (2002). RNA oligo was ligated at the decapped 5′-end of cleaved mRNA using T4 RNA ligase (New England Biolabs). Ligated mRNA was reverse transcribed using SuperScript III RT by using oligo DT primers to create RACE-ready first-strand cDNA with known priming sites at the 5′ and 3′ ends. This cDNA was amplified with 5′ and 3′ adapter-specific primers to obtain a population of cleaved products strictly ligated to both 5′ and 3′ adapters. For gene-specific cleaved product identification via RLM-RACE, the amplified PCR product of cDNA was used as a template for secondary PCR by adapter-specific and gene-specific primer sets. The final product was cloned and sequenced to obtain the specific site of cleavage. Sequences of all the oligonucleotides used in this study are listed in Supplemental Table S1.

Histochemical Staining and Imaging

For GUS staining, Arabidopsis seedlings with or without treatment were immersed in GUS staining solution (50 mM sodium phosphate buffer [pH 7.0], 2 mM EDTA, 0.12% [v/v] Triton, 0.4 mM ferrocyanide, 0.4 mM ferricyanide, and 1.0 mM 5-bromo-4-chloro-3-indoxyl-β-D-glucuronide cyclohexyl ammonium salt) and incubated in the dark at 37°C. Tissues were cleared by treatment with 70% ethanol at 65°C for 1 h and images were taken with a Nikon 80i microscope.

To visualize lignin deposition, seedlings were stained with basic fuchsin and calcofluor white solution (both from Sigma-Aldrich) for staining lignin and the cell wall boundary, respectively, as per the ClearSee protocol described by Ursache et al. (2018). After staining, roots were imaged with a LSM710 confocal microscope using 561 nm excitation and detection at 600–650 nm for basic fuchsin. The *CFP* image was captured with a confocal microscope at excitation wavelength 435 nm and emission wavelength scan range 450–490 nm with emission maxima at 477 nm. Callose staining was done as previously described by Müller et al. (2015). Seedlings were incubated in 150 mM K_2HPO_4 containing 0.01% aniline blue solution for 10 min and kept in the dark. After staining, seedlings were stored in 30% glycerol and callose deposition was visualized with a Nikon 80i fluorescence microscope using a UV filter. To visualize lignin deposition, seedlings were stained with freshly prepared 2% phloroglucinol (Sigma-Aldrich) solution (4:1, 20% ethanol:HCl) for 5 min. After staining with

phloroglucinol, roots were washed once with water and visualized with a Nikon 80i microscope.

For peroxidase activity, seedlings were immersed in 1 mg/mL DAB staining solution (1 mg/mL DAB solution, in 10 mM Na_2HPO_4, pH 3.0, and 0.05% Tween 20) for 10 min and staining solution was replaced with bleaching solution (ethanol:acetic acid:glycerol, 3:1:1, by volume) and incubated in a boiling water bath for 15 min. Samples were visualized with an AxioImager microscope (Zeiss).

The iron-specific Perls/DAB staining was done as described by Roschzttardtz et al. (2009). In brief, plants were incubated in Perls stain (4% [v/v] HCl and 4% [w/v] K-ferrocyanide) for 30 min. For DAB intensification, plants were washed with water and incubated for 1 h in methanol containing 10 mM Na-azide and 0.3% (v/v) H_2O_2 and washed with 100 mM Na-phosphate buffer (pH 7.4). Plants were incubated for 30 min in the intensification buffer containing 0.025% (w/v) DAB (Sigma-Aldrich) and 0.005% (v/v) H_2O_2. The reaction was stopped by washing with water and tissue was cleared with chloral hydrate (1 g/mL in 15% glycerol). Perls/DAB-stained roots were visualized with a Zeiss AxioImager microscope.

Lignin autofluorescence was visualized under simultaneous absorption of two 730-nm photons resulting in excitation at ~350–370 nm as described by Schuetz et al. (2014). Tissue clearing was done in 6:1 ethanol:acetic acid solution (by volume) for 24 h, washed twice with 95% ethanol, and gradually rehydrated using 70% ethanol, 30% ethanol, and water consecutively. Samples were subsequently mounted in chloral hydrate solution (9:1:3 chloral hydrate:glycerol:water [w/v/v]) and were imaged using a confocal microscope (Zeiss LSM510).

Guaiacol Peroxidase Assay

Guaiacol peroxidase (GPX) activity was measured according to the protocol of Egley et al. (1983) by monitoring the oxidation of guaiacol to tetraguaiacol at 470 nm. Each 3-mL reaction mixture consisted of 25 mM phosphate buffer (pH 7.0), 0.05% guaiacol, 0.1 mM EDTA, 1 mM H_2O_2, and 0.3 mL enzyme extract. The increase in absorbance was monitored spectrophotometrically for 5 min at 470 nm. The blank consisted of reaction mixture without enzyme extract. One unit of GPX was defined as the amount of enzyme that decomposes 1 μmol of guaiacol min^{-1} at 25°C. GPX activity was calculated using the extinction coefficient as 26.6 mM^{-1} cm^{-1}. Enzyme activity was expressed as units of activity per milligram of protein.

Total Lignin Content Estimation

Thioglycolic acid quantification of lignin was done according to Bonawitz et al. (2014). Briefly, ~100 mg of root tissue was homogenized in liquid nitrogen and extracted with 10 volumes of 100% methanol at 80°C for 2 h. Pellet was collected by centrifugation and washed with 10 volumes of water. Samples were suspended in 750 μL of water, 250 μL concentrated HCl, and 100 μL thioglycolic acid and incubated at 80°C for 3 h. Pellets were collected, washed with 1 mL of water and resuspended in 1 M NaOH followed by 12 h incubation at room temperature at 50 rpm. After incubation, Samples were centrifuged and the supernatant was transferred to a fresh tube with 200 μL concentrated HCl and incubated for 4 h at 4°C. Precipitation of this reaction was resuspended in 1 M NaOH and absorbance was determined at 280 nm by a spectrophotometer. Total lignin content was calculated using the standard thioglycolic acid-lignin (extinction coefficient $\varepsilon = 18.31$ cm^{-1} mg mL^{-1}). Lignin content was expressed as milligrams of lignothioglycolic acid (LTGA) per gram of tissue.

Accession Numbers

The Arabidopsis Information Resource accession numbers for the genes reported here are as follows: SALK_025690C (*lac2*), SAIL_292_B04 (*lac2*), AT1G18140 (*LAC1*), AT2G29130 (*LAC2*), AT2G30210 (*LAC3*), AT2G38080 (*LAC4*), AT2G40370 (*LAC5*), AT2G46570 (*LAC6*), AT3G09220 (*LAC7*), AT5G01040 (*LAC8*), AT5G01050 (*LAC9*), AT5G01190 (*LAC10*), AT5G03260 (*LAC11*), AT5G05390 (*LAC12*), AT5G07130 (*LAC13*), AT5G09360 (*LAC14*), AT5G48100 (*LAC15*), AT5G58910 (*LAC16*), AT5G60020 (*LAC17*), AT4G05105 (*Ath-miR397a*), AT4G13555 (*Ath-miR397b*), and At3g18780 (*AtACT2*).

Supplemental Data

The following supplemental materials are available.

Supplemental Figure S1. Expression analysis of *LACCASE* genes under 0.4 M mannitol treatment.

Supplemental Figure S2. Comparison of root phenotype, *LACCASE* gene expression, and peroxidase activity in roots of Col-0 and *lac2*.

Supplemental Figure S3. Tissue-specific promoter activity and expression of *miR397b* and *LAC2*, *LAC4*, and *LAC17* genes.

Supplemental Figure S4A. Design of the STTM construct and phenotype and expression of *LAC2* in multiple miR397bOX and STTM overexpressing Arabidopsis transgenic lines.

Supplemental Figure S4B. Phenotype and expression of *LAC2* in multiple *LAC2OX* and *rLAC2*-expressing Arabidopsis transgenic lines.

Supplemental Figure S5. Epistatic analysis of *miR397b* and *LAC2*.

Supplemental Figure S6. Comparison of root growth and expression of *LACCASE* genes in Col-0 and *lac2* under various low-Pi conditions.

Supplemental Figure S7. Lignin deposition in a root at early growth stage and *LAC2* promoter activity at the root tip.

Supplemental Figure S8. Root growth and lignin deposition in EZ of Col-0 and *lac2* seedlings upon treatment with different combinations of low Pi and iron.

Supplemental Table S1. List of oligonucleotides used in this study.

ACKNOWLEDGMENTS

The assistance of central instrumentation facilities of the NIPGR in various experiments is acknowledged. The authors acknowledge Dr. Sigal Savaldi Goldstein, Israel Institute of Technology-Technion, Haifa, for providing facilities for some experiments. H.K. acknowledges the India Council of Scientific and Industrial Research (CSIR) and NIPGR for a fellowship. The authors are thankful to DBT e-library Consortium (DeLCON) for providing access to e-resources.

Received July 25, 2019; accepted January 7, 2020; published January 16, 2020.

LITERATURE CITED

Abel S (2011) Phosphate sensing in root development. Curr Opin Plant Biol **14:** 303–309

Balzergue C, Dartevelle T, Godon C, Laugier E, Meisrimler C, Teulon JM, Creff A, Bissler M, Brouchoud C, Hagège A, et al (2017) Low phosphate activates STOP1-ALMT1 to rapidly inhibit root cell elongation. Nat Commun **8:** 15300

Bao Y, Aggarwal P, Robbins NE II, Sturrock CJ, Thompson MC, Tan HQ, Tham C, Duan L, Rodriguez PL, Vernoux T, et al (2014) Plant roots use a patterning mechanism to position lateral root branches toward available water. Proc Natl Acad Sci USA **111:** 9319–9324

Berthet S, Demont-Caulet N, Pollet B, Bidzinski P, Cézard L, Le Bris P, Borrega N, Hervé J, Blondet E, Balzergue S, et al (2011) Disruption of *LACCASE4* and *17* results in tissue-specific alterations to lignification of *Arabidopsis thaliana* stems. Plant Cell **23:** 1124–1137

Bloch D, Puli MR, Mosquna A, Yalovsky S (2019) Abiotic stress modulates root patterning via ABA-regulated *microRNA* expression in the endodermis initials. Development **146:** dev177097

Bohnert HJ, Nelson DE, Jensen RG (1995) Adaptations to environmental stresses. Plant Cell **7:** 1099–1111

Bonawitz ND, Kim JI, Tobimatsu Y, Ciesielski PN, Anderson NA, Ximenes E, Maeda J, Ralph J, Donohoe BS, Ladisch M, et al (2014) Disruption of Mediator rescues the stunted growth of a lignin-deficient *Arabidopsis* mutant. Nature **509:** 376–380

Boyer JS (1982) Plant productivity and environment. Science **218:** 443–448

Cai X, Davis EJ, Ballif J, Liang M, Bushman E, Haroldsen V, Torabinejad J, Wu Y (2006) Mutant identification and characterization of the laccase gene family in *Arabidopsis*. J Exp Bot **57:** 2563–2569

Chen C, Ridzon DA, Broomer AJ, Zhou Z, Lee DH, Nguyen JT, Barbisin M, Xu NL, Mahuvakar VR, Andersen MR, et al (2005) Real-time quantification of microRNAs by stem-loop RT-PCR. Nucleic Acids Res **33:** e179

Clough SJ, Bent AF (1998) Floral dip: A simplified method for *Agrobacterium*-mediated transformation of *Arabidopsis thaliana*. Plant J **16:** 735–743

Comas LH, Becker SR, Cruz VM, Byrne PF, Dierig DA (2013) Root traits contributing to plant productivity under drought. Front Plant Sci **4:** 442

de Gonzalo G, Colpa DI, Habib MHM, Fraaije MW (2016) Bacterial enzymes involved in lignin degradation. J Biotechnol **236:** 110–119

Driouich A, Laine´ AC, Vian B, Faye L (1992) Characterization and localization of laccase forms in stem and cell cultures of sycamore. Plant J **2:** 13–24

Egley GH, Paul RN Jr., Vaughn KC Jr., Duke SO (1983) Role of peroxidase in the development of water-impermeable seed coats in *Sida spinosa L.* Planta **157:** 224–232

Fan L, Linker R, Gepstein S, Tanimoto E, Yamamoto R, Neumann PM (2006) Progressive inhibition by water deficit of cell wall extensibility and growth along the elongation zone of maize roots is related to increased lignin metabolism and progressive stelar accumulation of wall phenolics. Plant Physiol **140:** 603–612

Fraser TE, Silk WK, Rost TL (1990) Effects of low water potential on cortical cell length in growing regions of maize roots. Plant Physiol **93:** 648–651

Freudenberg K (1959) Biosynthesis and constitution of lignin. Nature **183:** 1152–1155

Gutiérrez-Alanís D, Yong-Villalobos L, Jiménez-Sandoval P, Alatorre-Cobos F, Oropeza-Aburto A, Mora-Macías J, Sánchez-Rodríguez F, Cruz-Ramírez A, Herrera-Estrella L (2017) Phosphate starvation-dependent iron mobilization induces CLE14 expression to trigger root meristem differentiation through CLV2/PEPR2 signaling. Dev Cell **41:** 555–570

Hatfield R, Vermerris W (2001) Lignin formation in plants. The dilemma of linkage specificity. Plant Physiol **126:** 1351–1357

Hématy K, Sado PE, Van Tuinen A, Rochange S, Desnos T, Balzergue S, Pelletier S, Renou JP, Höfte H (2007) A receptor-like kinase mediates the response of Arabidopsis cells to the inhibition of cellulose synthesis. Curr Biol **17:** 922–931

Higuchi T (1985) Biosynthesis of lignin. In T Higuchi, ed, Biosynthesis and Biodegradation of Wood Components. Academic Press, New York, pp 141–160

Higuchi T, Ito Y (1958) Dehydrogenation products of coniferyl alcohol formed by the action of mushroom phenol oxidase, Rhus-laccase, and radish peroxidase. J Biochem **45:** 575–579

Jbir N, Chaïbi W, Ammar S, Jemmali A, Ayadi A (2001) Root growth and lignification of two wheat species differing in their sensitivity to NaCl, in response to salt stress. C R Acad Sci III **324:** 863–868

Kitin P, Voelker SL, Meinzer FC, Beeckman H, Strauss SH, Lachenbruch B (2010) Tyloses and phenolic deposits in xylem vessels impede water transport in low-lignin transgenic poplars: A study by cryo-fluorescence microscopy. Plant Physiol **154:** 887–898

Lee DK, Jung H, Jang G, Jeong JS, Kim YS, Ha SH, Do Choi Y, Kim JK (2016) Overexpression of the OsERF71 transcription factor alters rice root structure and drought resistance. Plant Physiol **172:** 575–588

Lee Y, Rubio MC, Alassimone J, Geldner N (2013) A mechanism for localized lignin deposition in the endodermis. Cell **153:** 402–412

Liu CJ, Miao YC, Zhang KW (2011) Sequestration and transport of lignin monomeric precursors. Molecules **16:** 710–727

Livak KJ, Schmittgen TD (2001) Analysis of relative gene expression data using real-time quantitative PCR and the $2^{-\Delta\Delta CT}$ method. Methods **25:** 402–408

Llave C, Xie Z, Kasschau KD, Carrington JC (2002) Cleavage of *Scarecrow*-like mRNA targets directed by a class of *Arabidopsis* miRNA. Science **297:** 2053–2056

López-Bucio J, Hernández-Abreu E, Sánchez-Calderón L, Nieto-Jacobo MF, Simpson J, Herrera-Estrella L (2002) Phosphate availability alters architecture and causes changes in hormone sensitivity in the *Arabidopsis* root system. Plant Physiol **129:** 244–256

Lu C, Meyers BC, Green PJ (2007) Construction of small RNA cDNA libraries for deep sequencing. Methods **43:** 110–117

Lu S, Li Q, Wei H, Chang MJ, Tunlaya-Anukit S, Kim H, Liu J, Song J, Sun YH, Yuan L, et al (2013) Ptr-miR397a is a negative regulator of laccase genes affecting lignin content in *Populus trichocarpa*. Proc Natl Acad Sci USA **110:** 10848–10853

Maia JM, Voigt EL, Ferreira-Silva SL, Fontenele AV, Maĉedo EC, Silveira JAG (2013) Differences in cowpea root growth triggered by salinity and dehydration are associated with oxidative modulation involving types I and II peroxidases and apoplastic ascorbate. J Plant Growth Regul **32:** 376–387

McDougall GJ (2000) A comparison of proteins from the developing xylem of compression and non-compression wood of branches of sitka spruce (*Picea sitchensis*) reveals a differentially expressed laccase. J Exp Bot **51:** 1395–1401

Merz D, Richter J, Gonneau M, Sanchez-Rodriguez C, Eder T, Sormani R, Martin M, Hématy K, Höfte H, Hauser MT (2017) T-DNA alleles of the receptor kinase THESEUS1 with opposing effects on cell wall integrity signaling. J Exp Bot **68:** 4583–4593

Mir Derikvand M, Sierra JB, Ruel K, Pollet B, Do CT, Thévenin J, Buffard D, Jouanin L, Lapierre C (2008) Redirection of the phenylpropanoid pathway to feruloyl malate in *Arabidopsis* mutants deficient for cinnamoyl-CoA reductase 1. Planta **227:** 943–956

Mitsuda N, Iwase A, Yamamoto H, Yoshida M, Seki M, Shinozaki K, Ohme-Takagi M (2007) NAC transcription factors, NST1 and NST3, are key regulators of the formation of secondary walls in woody tissues of *Arabidopsis*. Plant Cell **19:** 270–280

Mitsuda N, Seki M, Shinozaki K, Ohme-Takagi M (2005) The NAC transcription factors NST1 and NST2 of *Arabidopsis* regulate secondary wall thickenings and are required for anther dehiscence. Plant Cell **17:** 2993–3006

Moubayidin L, Perilli S, Dello Ioio R, Di Mambro R, Costantino P, Sabatini S (2010) The rate of cell differentiation controls the *Arabidopsis* root meristem growth phase. Curr Biol **20:** 1138–1143

Müller J, Toev T, Heisters M, Teller J, Moore KL, Hause G, Dinesh DC, Bürstenbinder K, Abel S (2015) Iron-dependent callose deposition adjusts root meristem maintenance to phosphate availability. Dev Cell **33:** 216–230

Nilsson R, Bernfur K, Gustavsson N, Bygdell J, Wingsle G, Larsson C (2010) Proteomics of plasma membranes from poplar trees reveals tissue distribution of transporters, receptors, and proteins in cell wall formation. Mol Cell Proteomics **9:** 368–387

Péret B, Clément M, Nussaume L, Desnos T (2011) Root developmental adaptation to phosphate starvation: Better safe than sorry. Trends Plant Sci **16:** 442–450

Pritchard J (1994) The control of cell expansion in roots. New Phytol **127:** 3–26

Raghothama KG (1999) Phosphate acquisition. Annu Rev Plant Physiol Plant Mol Biol **50:** 665–693

Ramachandran P, Wang G, Augstein F, de Vries J, Carlsbecker A (2018) Continuous root xylem formation and vascular acclimation to water deficit involves endodermal ABA signalling via miR165. Development **145:** dev159202

Ranocha P, Chabannes M, Chamayou S, Danoun S, Jauneau A, Boudet AM, Goffner D (2002) Laccase down-regulation causes alterations in phenolic metabolism and cell wall structure in poplar. Plant Physiol **129:** 145–155

Ranocha P, McDougall G, Hawkins S, Sterjiades R, Borderies G, Stewart D, Cabanes-Macheteau M, Boudet AM, Goffner D (1999) Biochemical characterization, molecular cloning and expression of laccases—a divergent gene family—in poplar. Eur J Biochem **259:** 485–495

Reina JJ, Domínguez E, Heredia A (2001) Water sorption-desorption in conifer cuticles: The role of lignin. Physiol Plant **112:** 372–378

Reinhammar B, Malmstroem BG (1981) "Blue" copper-containing oxidases. In TG Spiro, ed, Copper Proteins, Vol **Vol 3**. Wiley, New York, pp 109–149

Richardson A, Duncan J, McDougall GJ (2000) Oxidase activity in lignifying xylem of a taxonomically diverse range of trees: Identification of a conifer laccase. Tree Physiol **20:** 1039–1047

Ros Barceló A (1997) Lignification in plant cell walls. Int Rev Cytol **176:** 87–132

Rosas-Cárdenas F, Durán-Figueroa N, Vielle-Calzada JP, Cruz-Hernández A, Marsch-Martínez N, de Folter S (2011) A simple and efficient method for isolating small RNAs from different plant species. Plant Methods **7:** 4

Roschzttardtz H, Conéjéro G, Curie C, Mari S (2009) Identification of the endodermal vacuole as the iron storage compartment in the *Arabidopsis* embryo. Plant Physiol **151:** 1329–1338

Sarkanen KV (1971) Lignin precursors and their polymerization. *In* KV Sarkanen, and CH Ludwig, eds, Lignins: Occurrence, Formation, Structure and Reactions. Wiley-Interscience, New York, pp 95–163

Schneider CA, Rasband WS, Eliceiri KW (2012) NIH Image to ImageJ: 25 years of image analysis. Nat Methods **9:** 671–675

Schuetz M, Benske A, Smith RA, Watanabe Y, Tobimatsu Y, Ralph J, Demura T, Ellis B, Samuels AL (2014) Laccases direct lignification in the discrete secondary cell wall domains of protoxylem. Plant Physiol **166:** 798–807

Sharp RE, Silk WK, Hsiao TC (1988) Growth of the maize primary root at low water potentials: I. Spatial distribution of expansive growth. Plant Physiol **87:** 50–57

Sinclair TR, Muchow RC (2001) System analysis of plant traits to increase grain yields on limited water supplies. Agron J **93:** 263–270

Singh AP, Fridman Y, Friedlander-Shani L, Tarkowska D, Strnad M, Savaldi-Goldstein S (2014) Activity of the brassinosteroid transcription factors BRASSINAZOLE RESISTANT1 and BRASSINOSTEROID INSENSITIVE1-ETHYL METHANESULFONATE-SUPPRESSOR1/BRASSINAZOLE RESISTANT2 blocks developmental reprogramming in response to low phosphate availability. Plant Physiol **166:** 678–688

Singh AP, Fridman Y, Holland N, Ackerman-Lavert M, Zananiri R, Jaillais Y, Henn A, Savaldi-Goldstein S (2018) Interdependent nutrient availability and steroid hormone signals facilitate root growth plasticity. Dev Cell **46:** 59–72.e4

Sunkar R, Zhu JK (2004) Novel and stress-regulated microRNAs and other small RNAs from *Arabidopsis*. Plant Cell **16:** 2001–2019

Svistoonoff S, Creff A, Reymond M, Sigoillot-Claude C, Ricaud L, Blanchet A, Nussaume L, Desnos T (2007) Root tip contact with low-phosphate media reprograms plant root architecture. Nat Genet **39:** 792–796

Takahama U (1995) Oxidation of hydroxycinnamic acid and hydroxycinnamyl alcohol derivatives by laccase and peroxidase. Interactions among *p*-hydroxyphenyl, guaiacyl and syringyl groups during the oxidation reactions. Physiol Plant **93:** 61–68

Takeba G, Matsubara S (1979) Measurement of growth potential of the embryo in New York lettuce seed under various combinations of temperature, red light and hormones. Plant Cell Physiol **20:** 51–61

Toufighi K, Brady SM, Austin R, Ly E, Provart NJ (2005) The Botany Array Resource: e-northerns, expression angling, and promoter analyses. Plant J **43:** 153–163

Tyree MT, Davis SD, Cochard H (1994) Biophysical perspectives of xylem evolution: Is there a tradeoff of hydraulic efficiency for vulnerability to dysfunction? IAWA J **15:** 335–360

Ursache R, Andersen TG, Marhavý P, Geldner N (2018) A protocol for combining fluorescent proteins with histological stains for diverse cell wall components. Plant J **93:** 399–412

Vadez V (2014) Root hydraulics: The forgotten side of roots in drought adaptation. Field Crops Res **165:** 15–24

Valladares F, Gianoli E, Gómez JM (2007) Ecological limits to plant phenotypic plasticity. New Phytol **176:** 749–763

van Kleunen M, Fischer M (2005) Constraints on the evolution of adaptive phenotypic plasticity in plants. New Phytol **166:** 49–60

Vanholme R, Demedts B, Morreel K, Ralph J, Boerjan W (2010) Lignin biosynthesis and structure. Plant Physiol **153:** 895–905

Varkonyi-Gasic E, Wu R, Wood M, Walton EF, Hellens RP (2007) Protocol: A highly sensitive RT-PCR method for detection and quantification of microRNAs. Plant Methods **3:** 12

Verslues PE, Agarwal M, Katiyar-Agarwal S, Zhu J, Zhu JK (2006) Methods and concepts in quantifying resistance to drought, salt and freezing, abiotic stresses that affect plant water status. Plant J **45:** 523–539

Wang CY, Zhang S, Yu Y, Luo YC, Liu Q, Ju C, Zhang YC, Qu LH, Lucas WJ, Wang X, et al (2014) MiR397b regulates both lignin content and seed number in Arabidopsis via modulating a laccase involved in lignin biosynthesis. Plant Biotechnol J **12:** 1132–1142

Ward JT, Lahner B, Yakubova E, Salt DE, Raghothama KG (2008) The effect of iron on the primary root elongation of Arabidopsis during phosphate deficiency. Plant Physiol **147:** 1181–1191

Yamamura M, Noda S, Hattori T, Shino A, Kikuchi J, Takabe K, Tagane S, Gau M, Uwatoko N, Mii M, et al (2013) Characterization of lignocellulose of *Erianthus arundinaceus* in relation to enzymatic saccharification efficiency. Plant Biotechnol **30:** 25–35

Yan J, Gu Y, Jia X, Kang W, Pan S, Tang X, Chen X, Tang G (2012) Effective small RNA destruction by the expression of a short tandem target mimic in *Arabidopsis*. Plant Cell **24:** 415–427

Yang L, Wang CC, Guo WD, Li XB, Lu M, Yu CL (2006) Differential expression of cell wall related genes in the elongation zone of rice roots under water deficit. Russ J Plant Physiol **53:** 390–395

Youn HD, Hah YC, Kang SA (1995) Role of laccase in lignin degradation by white-rot fungi. FEMS Microbiol Lett **132:** 183–188

Zhao Q, Nakashima J, Chen F, Yin Y, Fu C, Yun J, Shao H, Wang X, Wang ZY, Dixon RA (2013) Laccase is necessary and nonredundant with peroxidase for lignin polymerization during vascular development in *Arabidopsis*. Plant Cell **25:** 3976–3987

Zhou C, Li Q, Chiang VL, Lucia LA, Griffis DP (2011) Chemical and spatial differentiation of syringyl and guaiacyl lignins in poplar wood via time-of-flight secondary ion mass spectrometry. Anal Chem **83:** 7020–7026

Ziegler J, Schmidt S, Chutia R, Müller J, Böttcher C, Strehmel N, Scheel D, Abel S (2016) Non-targeted profiling of semi-polar metabolites in *Arabidopsis* root exudates uncovers a role for coumarin secretion and lignification during the local response to phosphate limitation. J Exp Bot **67:** 1421–1432

Zimmermann MN (1983) Xylem Structure and the Ascent of Sap. *In* TE Timell, ed, Springer Series in Wood Science. Springer-Verlag, Berlin, pp 66–68